SANC integrator in the progress: QCD and EW contributions

D. Bardin[+1)], S. Bondarenko[*], P. Christova[+], L. Kalinovskaya[+], L. Rumyantsev[+×], A. Sapronov[+],
W. von Schlippe[°]

[+]*Dzhelepov Laboratory for Nuclear Problems, Joint Institute for Nuclear Research, 141980 Dubna, Russia*

[*]*Bogoliubov Laboratory of Theoretical Physics, Joint Institute for Nuclear Research, 141980 Dubna, Russia*

[×]*Institute of Physics, Southern Federal University, 344090 Rostov-on-Don, Russia*

[°]*Konstantinov Petersburg Nuclear Physics Institute of the RAS, 188300 Gatchina, Russia*

Submitted 19 July 2012

Modules and packages for the one-loop calculations at partonic level represent the first level of SANC output computer product. The next level represents Monte Carlo integrator `mcsanc`, realizing fully differential hadron level calculations (convolution with PDF) for the HEP processes at LHC. In this paper we describe the implementation into the framework `mcsanc` first set of processes: DY NC, DY CC, $f_1 \bar{f}_1' \to HW^{\pm}(Z)$ and single top production. Both EW and QCD NLO corrections are taken into account. A comparison of SANC results with those existing in the world literature is given.

1. Introduction. Recent reviews of theoretical predictions and their uncertainties for basic LHC processes in the Standard Model (SM) can be found in Rep. [1, 2].

The interpretation of high-quality data of the LHC demands an equally high precision in the theoretical predictions at the level of quantum corrections. Apart from a detailed knowledge of higher-order EW and QCD corrections, the combination of their effects must be investigated. Advanced computational tools were developed to control the interplay of EW and QCD corrections: [3–7].

In this paper new results of the computer system SANC (Support of Analytic and Numerical Calculations for experiments at Colliders) [8] are presented. In this system it is possible to achieve the one loop level predictions in the EW and QCD sectors on the same platform of the analytic procedures.

The first level of the computer products SANC are: analytical modules for scalar Form Factors (FF) and Helicity Amplitudes (HA) and accompanying bremsstrahlung contributions (BR or MC) and the `s2n.f` package producing the FORTRAN codes [9].

In this paper we discuss in some detail the results of the implementation at hadronic level in the newly developed `mcsanc-1.0` integrator[2)], based on the above mentioned modules. The processes are marked by process identifiers: pid=cnn, c=charge: 0-NC, ±-CC, and: nn=01(e), 02(μ), 03(τ) etc, see below.

- Drell−Yan-like single W production: pid $= \pm 102$

$$\bar{d} + u \to l^+ + \nu_l. \tag{1}$$

- Drell−Yan-like single Z production: pid $= 002$

$$q + \bar{q} \to l^+ + l^-. \tag{2}$$

- $HW^{\pm}(Z)$ production: pid $= \pm 104$ (004).
At the parton level we consider

$$f_1 \bar{f}_1' HW^{\pm}(Z) \to 0 \tag{3}$$

(where f_1 stands for a *massless fermion* of the SM, while specifically for bosons we use Z, $W^{\pm}$, H). It should be emphasized also that the notation $ffHW \to 0$ means that all external 4-momenta flow inwards; this is the standard SANC convention which allows to compute one-loop covariant amplitude (CA) and form factors (FF) only once and obtain CA for a specific channel by means of a crossing transformation.

- The s and t channels of single top quark production: pid $= \pm 105(s), \pm 106(t)$

$$t\bar{b}\bar{u}d \to 0 \quad \text{and} \quad \bar{t}bu\bar{d} \to 0. \tag{4}$$

Previous studies of these processes by SANC system, i.e. creation of the analytic platform and modules at the parton level were presented in [8–15].

The paper is organized as follows. First, an overview of the `mcsanc-1.0` integrator is given in section 2. In subsection 2.1 we describe a list of contributions to hard sub-processes and introduce their enumeration. Then we describe the parallel calculations issue. Section 3 contains numerical results for the processes in QCD and

---

[1)] e-mail: sanc@jinr.ru

[2)] The package can be downloaded from SANC homepages: `sanc.jinr.ru` and `pcphsanc.cern.ch`.

EW sectors. Input parameters, kinematical cuts, and the used PDFs can be found in subsection 3.1. Further, we present the complete predictions for inclusive cross sections at LO and NLO levels in the EW and QCD sectors for processes (1)–(4). We systematically compare our results for NLO QCD corrections with the program MCFM [16, 17] and, whenever possible, with other codes existing in the literature: [18, 19] (EW) and [20] (QCD).

In section 4 we summarize our results.

2. Sanc integrator.

2.1. *Description of* `id`*'s for hard sub-processes.* At NLO level several hard sub-processes contribute to a given process. In general, it consists of several parts: LO – lowest order, Virt – virtual, Real – real brems(glue)strahlung and Subt – subtraction; Real, in turn, is subdivided into Soft and Hard contributions. We enumerate them through `id = 0 − 6`:

id0:   LO, $2 \rightarrow 2$, tree-level, $q\bar{q}'$ NC or CC sub-processes.

id1:   Subt term responsible for the subtraction of the initial quark mass (m_q) singularities for $q\bar{q}'$ sub-processes, computed in a given subtraction scheme ($\overline{\text{MS}}$ or DIS). It depends on $\ln(m_q)$.

id2:   Virt represents only the NLO EW parts, stands for pure EW one-loop virtual contributions. It depends on m_q and may depend on an infrared regulator (e.g. on an infinitesimal photon mass). It is not present for QCD NLO contributions, where it is added to the soft contribution (see next item). For DY NC NLO EW process it contains all virtual contributions, both EW and QED.

id3:   For all processes, except DY NC, this stands for the sum of Virt and Real Soft (QED/QCD) contributions, therefore it does not depend on the infrared regulator but depends on m_q and on the soft-hard separator $\bar{\omega}$. For DY NC NLO EW processes it is just the Real Soft QED contribution that depends on the infrared regulator, on m_q and on the soft-hard separator $\bar{\omega}$.

id4:   For all processes this is just the Real Hard (QED/QCD) contribution that depends on m_q and on $\bar{\omega}$.

id5:   Subt term is responsible for the subtraction of the initial quark mass singularities for $gq(gq')$ sub-processes (also computed in $\overline{\text{MS}}$ or DIS schemes). It contains logarithmic singularities in m_q.

id6:   The gluon-induced sub-process – an analog of `id4` for $gq(gq')$ sub-processes. They also contain loga-

rithmic mass singularities which cancel those from `id5`.

The quark mass is used to regularize the collinear divergences, the soft-hard separator is a remainder of infrared divergences. The sum of contributions with `id3` and `id4` is independent of $\bar{\omega}$. The sums `id1+id2+id3+id4` and `id5+id6` are separately independent of m_q. Therefore, the entire NLO sub-process is independent of both unphysical parameters $\bar{\omega}$ and m_q.

2.2. *Parallel calculations.* The `mcsanc` program takes advantage of parallelization in the Cuba library [21, 22], used as a Monte-Carlo integrating tool. However, the parallelization efficiency is reduced by the overhead of inter-process communications.

Figure 1 shows time required to complete the NLO EW cross section calculation depending on the number
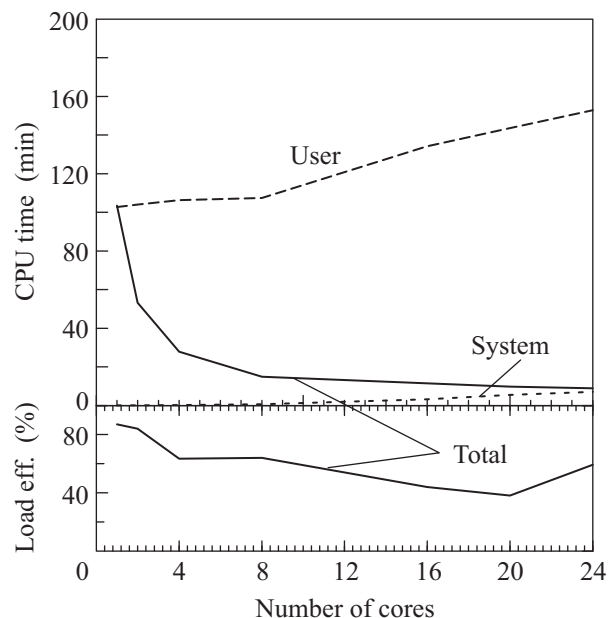

Fig. 1. CPU usage and load efficiency for the `mcsanc` program depending on the number of processor cores

of active CPU cores. The test was run on a dual-processor Intel ® Xeon ® machine with 12 real (24 virtual) cores with Linux operating system. The upper plot summarizes multicore CPU productivity: "total" is the wall clock time passed during the run; "user" is the CPU time consumed by the program (roughly equals to wall clock time multiplied by the number of cores in case of 100% efficiency); "system" is the time spent by the operating system on multiprocessing service.

One can see that the parallelization is efficient with number of cores up to 8, after which the total run time does not significantly decrease and the overhead CPU time ("user") grows. It is also apparent from the lower

plot that the average CPU load efficiency drops below 50% with more than 8 cores active.

3. Numerical results. In this section the results obtained by the `mcsanc` integrator realizing fully differential hadron level calculations for the processes (1)–(4) are presented.

We produce comparison with numerical results for the NLO QCD corrections for all our processes between SANC and [16]. For the NLO electroweak corrections for Drell–Yan NC and CC processes (pid = 002, ±102) this was done early within the workshop [23]. For WH production, i.e. pid = ±104, in EW sector between SANC and [18] and in QCD sector between SANC and [20] for pid = ±105, ±106.

3.1. *Setup: PDF, cuts, input parameters.* For the numerical results in this section we have used the following setup.

• PDF set, scales, α_s. We use `CT10(f[scale])` PDF from the LHAPDF library and compute α_s via a call to `alphasPDF(r[scale])`. Usually we set factorization scale (`fscale`) equal to renormalization scale (`rscale`) and different for the processes under consideration: M_V for DY-like single V production; M_{V+H} for the processes Eq. (3); m_t for the processes Eq. (4).

• Phase-space cuts. We use loose cuts: for the final state particle transverse momenta $p_T \geq 0.1\,\text{GeV}$, no cuts for their rapidities and for the neutral current DY, in addition, $M_{l+l-} \geq 20\,\text{GeV}$. We demonstrate numerical results for Drell–Yan only for muon case and we are not dealing with effects of recombination. We choose $\omega = 10^{-4}$ and the cms energy $\sqrt{s_0} = 14\,\text{TeV}$ if not stated otherwise.

• Set of EW scheme and input parameters. We choose the G_μ EW scheme, and input parameters are taken from PDG-2011 (on 16/05/2012):
Coupling constants: $\alpha = 1/137.035999679$, $G_F = 1.16637 \cdot 10^{-5}$. Boson masses: $M_W = 80.399\,\text{GeV}$, $M_Z = 91.1876\,\text{GeV}$, $M_H = 120\,\text{GeV}$. Boson widths: $\Gamma_Z = 2.4952\,\text{GeV}$, $\Gamma_W = 2.085\,\text{GeV}$. CKM matrix: $V_{ud} = 0.9738$, $V_{us} = 0.2272$, $V_{cd} = 0.2271$, $V_{cs} = 0.9730$. Lepton masses: $m_e = 0.510998910\,\text{MeV}$, $m_\mu = 0.105658367\,\text{GeV}$, $m_\tau = 1.77682\,\text{GeV}$. Heavy quark masses: $m_b = 4.67\,\text{GeV}$, $m_t = 172.9\,\text{GeV}$. Masses of the four light quarks are taken from [24]: $m_d = 0.066\,\text{GeV}$, $m_u = 0.066\,\text{GeV}$, $m_s = 0.150\,\text{GeV}$, $m_c = 1.2\,\text{GeV}$.

3.2. *Example of $M_{\mu+\mu-}$ distributions, DY NC.* The standard ATLAS Monte Carlo (MC) generation uses the PYTHIA–PHOTOS chain of programs. PYTHIA [25, 26] has the leading order (LO) matrix element for a given process and takes into account Parton Showers (PS); PHOTOS [27–29] describes multiphoton emission from the Final State (FSR) di-lepton system. This procedure

does not include certain next-to-leading order (NLO) EW corrections, like Pure Weak (PW) contributions, Initial–Final QED interference (IFI) and what remains from Initial State Radiation (ISR) after subtraction of collinear divergences. In SANC one can evaluate the entire effect of these corrections as a difference of complete NLO EW corrections and the QED FSR corrections. See, for example, the distribution of the complete NLO EW corrections over Z boson invariant mass, $\delta(M_{\mu+\mu-})$, for Drell–Yan-like single Z production around Z resonance, ($\delta = (d\sigma^{\text{NLO}}/dM_{\mu+\mu-})/(d\sigma^{\text{LO}}/dM_{\mu+\mu-}) - 1$ and with taking into account only QED FSR corrections, Fig. 2.
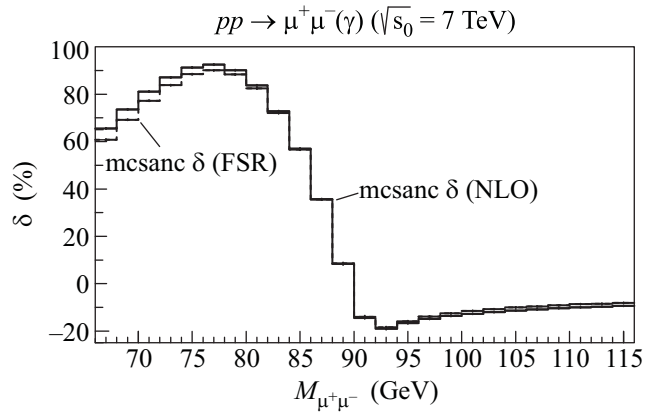
Fig. 2. δ in % with complete NLO EW (solid histogram) and FSR (dashed histogram) corrections

NLO and FSR distributions in Fig. 2 are barely distinguishable. The difference $\delta^{\text{Diff}} = \delta^{\text{NLO−FSR}}(M_{\mu+\mu-})$ is shown in Fig. 3.
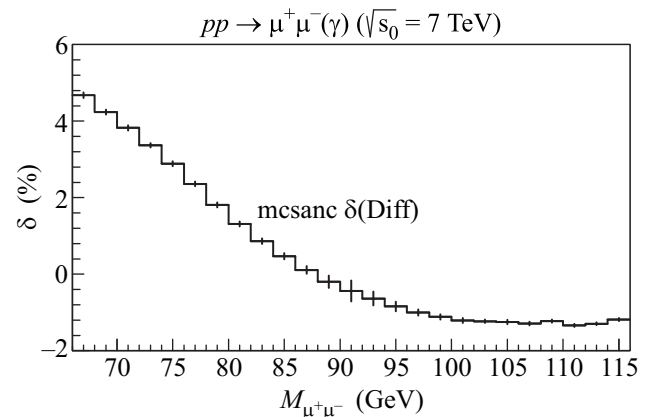
Fig. 3. Difference correction δ^{Diff} in % for the distribution over $M_{\mu+\mu-}$

As is seen, for the $M_{\mu+\mu-}$ interval around the Z resonance, δ^{Diff} varies from +5% at the lower edge to −1%

at the upper edge and therefore cannot be neglected, if the precision tag is equal to 1%, say.

3.3. *Numerical results and comparison for LO, NLO EW, NLO QCD RC.*

● In Tables 1–3 we present LO and NLO inclusive cross sections for processes (1), (2), (3) and (4), respectively.

Table 1

NC and CC DY processes, i.e. for pid $= 002, \pm 102$. LO, NLO EW, NLO QCD cross sections are given in picobarns and compared with corresponding values obtained with the aid of the program MCFM. Also correction factors are shown in %. The numbers illustrate good agreement within statistical errors of MC integration

Pid	002	102	−102
LO	3338(1)	10696(1)	7981(1)
LO MCFM	3338(1)	10696(1)	7981(1)
NLO QCD	3388(2)	12263(4)	9045(4)
NLO MCFM	3382(1)	12260(1)	9041(5)
δ_{QCD}	1.49(3)	14.66(1)	13.35(3)
NLO EW	3345(1)	10564(1)	7861(1)
δ_{EW}	0.22(1)	−1.23(1)	−1.49(1)

Table 2

The same as in Table 1 but for processes of $HZ(W^{\pm})$ production, i.e. pid $= 004, \pm 104$

Pid	004	104	−104
LO	0.8291(1)	0.9277(1)	0.5883(1)
LO MCFM	0.8292(1)	0.9280(2)	0.5885(1)
NLO QCD	0.9685(3)	1.0897(3)	0.6866(3)
NLO MCFM	0.9686(1)	1.0901(2)	0.6870(1)
δ_{QCD}	16.81(3)	17.47(3)	16.72(5)
NLO EW	0.7877(1)	0.8672(2)	0.5508(1)
δ_{EW}	−5.00(2)	−6.52(2)	−6.38(3)

● In Table 4 we show QCD and EW cross section contributions to the processes of HW$^{\pm}$ production, pid $= \pm 104$, detailed over id's of the `mcsanc` integrator. As is seen for the chosen setup (Subsection 3.1) there is strong cancellation of the Soft and Hard contributions id's=3,4 and gluon induced contributions id's=5,6, the sum of contributions id's=5+6 being negative. We remind that the sum of all contributions is independent of the unphysical parameters $\bar{\omega}$ and m_q.

● The other comparisons.

1. EW corrections: a comparison of EW and QCD NLO corrections between `mcsanc` and papers [18, 19] was done using corresponding setup. We received good

Table 3

The same as in Table 1 but for single top, *s* and *t* channels, i.e. for pid $= \pm 105, \pm 106$

Pid	105	−105
LO	5.134(1)	3.205(1)
LO MCFM	5.133(1)	3.203(1)
NLO QCD	6.921(2)	4.313(2)
NLO MCFM	6.923(2)	4.309(1)
δ_{QCD}	34.79(5)	34.56(8)
NLO EW	5.022(1)	3.140(1)
δ_{EW}	−2.18(1)	−2.02(2)

Pid	106	−106
LO	158.73(2)	95.18(2)
LO MCFM	158.69(7)	95.27(4)
NLO QCD	152.13(9)	90.44(7)
NLO MCFM	152.07(14)	90.50(8)
δ_{QCD}	−4.17(6)	−4.08(8)
NLO EW	164.44(5)	98.65(4)
δ_{EW}	3.59(3)	3.66(5)

Table 4

EW and QCD radiative corrections in picobarns detailed over id's for pid $= \pm 104$, parameter $\bar{\omega} = 10^{-4}$

QCD	Pid	104	−104
	id0	0.9277(1)	0.5883(1)
	id1	0.6916(1)	0.4860(1)
	id3	−10.9233(1)	−6.9139(1)
	id4	10.4547(1)	6.5737(1)
	id5	−0.9717(1)	−0.6733(1)
	id6	0.9107(1)	0.6258(1)
	NLO QCD	1.0897(3)	0.6866(3)
EW	Pid	104	−104
	id0	0.9277(1)	0.5884(1)
	id1	0.0100(1)	0.0070(0)
	id2	−0.0560(0)	−0.0349(0)
	id3	−0.1592(1)	−0.1003(0)
	id4	0.1448(1)	0.0907(1)
	NLO EW	0.8672(2)	0.5508(1)

agreement within statistical errors with the results presented in the references.

2. QCD corrections: a comparison between inclusive LO and NLO cross sections from `mcsanc` and Table 1 of paper [20] was carried out using tuned setup. Agreement within MC errors was found for LO, while for NLO only a qualitative agreement was reached, since we did not manage to reproduce the corresponding value for $\alpha_s(r)$.

More comparisons including differential distributions (as in papers [4, 30]) will be presented elsewhere.

4. Conclusions. To match the experimental accuracy at the LHC, we direct our effort to developing a programming environment for the calculation of processes at one loop level and to creating the `mcsanc` integrator with EW and QCD branches at hadron level.

In this paper we have presented results for EW and QCD corrections to the following processes: Z and W production, HZ and $HW^{\pm}$ production, and single top production processes. Our investigation confirms that NLO precision level and combination of EW and QCD corrections are mandatory for the precision tag of the LHC experiments.

1. S. Dittmaier, C. Mariotti, G. Passarino et al. (LHC Higgs Cross Sections Working Group Collaboration), 1201.3084.

2. S. Dittmaier et al. (LHC Higgs Cross Sections Working Group Collaboration), 1101.0593.

3. G. Balossini, G. Montagna, C. M. Carloni Calame et al., JHEP **1001**, 013 (2010); 0907.0276.

4. A. Denner, S. Dittmaier, S. Kallweit, and A. Muck, JHEP **1203**, 075 (2012); 1112.5142.

5. C. Bernaciak and D. Wackeroth, Phys. Rev. D **85**, 093003 (2012); 1201.4804.

6. L. Barze, G. Montagna, P. Nason et al., JHEP **1204**, 037 (2012); 1202.0465.

7. S. Yost, V. Halyo, M. Hejna, and B. Ward, 1201.5906.

8. A. Andonov, A. Arbuzov, D. Bardin et al., Comput. Phys. Commun. **174**, 481 (2006); hep-ph/0411186.

9. A. Andonov, A. Arbuzov, D. Bardin et al., Comput. Phys. Commun. **181**, 305 (2010); 0812.4207.

10. A. Arbuzov, D. Bardin, S. Bondarenko et al, Eur. Phys. J. C **46**, 407 (2006); hep-ph/0506110.

11. A. Arbuzov, D. Bardin, S. Bondarenko et al., Eur. Phys. J. C **51**, 585 (2007); hep-ph/0703043.

12. A. Arbuzov, D. Bardin, S. Bondarenko et al, Eur. Phys. J. C **54**, 451 (2008); 0711.0625.

13. A. Andonov, A. Arbuzov, S. Bondarenko et al., Phys. Atom. Nucl. **73**, 1761 (2010); 0901.2785.

14. D. Bardin, S. Bondarenko, L. Kalinovskaya et al., Eur. Phys. J. C **71**, 1533 (2011); 1008.1859.

15. D. Bardin, S. Bondarenko, P. Christova et al., 1110.3622.

16. J. M. Campbell and R. K. Ellis, arXiv/1007.3492.

17. J. Campbell, K. Ellis, and C. Williams, http://mcfm.fnal.gov/.

18. M. Ciccolini, S Dittmaier, and M. Kramer, Phys. Rev. D **68**, 073003 (2003); hep-ph/0306234.

19. O. Brein, M. Ciccolini, S. Dittmaier et al., hep-ph/0402003.

20. B. Harris, E. Laenen, L. Phaf et al., Phys. Rev. D **66**, 054024 (2002); hep-ph/0207055.

21. T. Hahn, Comput. Phys. Commun. **168**, 78 (2005); hep-ph/0404043.

22. T. Hahn, Cuba – a library for multidimensional numerical integration: www.feynarts.de/cuba/.

23. C. Buttar, J. D'Hondt, M. Kramer et al., 0803.0678.

24. S. Dittmaier and M. Huber, JHEP **1001**, 060 (2010); 0911.2329.

25. T. Sjostrand, S. Mrenna, and P. Skands, JHEP **0605**, 026 (2006); hep-ph/0603175.

26. T. Sjostrand, S. Mrenna, and P. Skands, Comput. Phys. Commun. **178**, 852 (2008); 0710.3820.

27. E. Barberio, B. van Eijk, and Z. Was, Comput. Phys. Commun. **66**, 115 (1991).

28. P.Golonka and Z. Was, Eur. Phys. J. C **45**, 97(2006); hep-ph/0506026.

29. Z. Was, P. Golonka, and G. Nanava, Nucl. Phys. Proc. Suppl. **181–182**, 269 (2008); 0807.2762.

30. A. Denner, S. Dittmaier, S. Kallweit, and A. Muck, 1112.5258.